Journal of Solid State Chemistry 183 (2010) 1394–1399

Contents lists available at ScienceDirect

Journal of Solid State Chemistry

journal homepage: www.elsevier.com/locate/jssc

Synthesis and photocatalytic activity of co-doped mesoporous TiO_2 on Brij98/CTAB composite surfactant template

Xiaotong Zhang, Guowei Zhou *, Jing Xu, Guangwei Bai, Lei Wang

School of Chemical Engineering, Shandong Institute of Light Industry, and Key Laboratory for Fine Chemicals of Shandong Province, Jinan, 250353 Shandong, PR China

ARTICLE INFO

Article history:
Received 14 January 2010
Received in revised form
1 March 2010
Accepted 10 April 2010

Keywords:
Mesoporous TiO_2
Brij98
CTAB
Photocatalysis
Papermaking wastewater
$CODc_r$

ABSTRACT

Using composite surfactant templates, polyoxyethylene (20) oleyl ether (Brij98) and cetyl trimethyl ammonium bromide (CTAB), as structure-directing agents, N and La co-doped mesoporous TiO_2 complex photocatalysts were synthesized successfully. The micromorphology of co-doped mesoporous TiO_2 samples was characterized by X-ray diffraction (XRD), transmission electron microscopy (TEM), Fourier transformed infrared spectroscopy (FT-IR), energy-dispersive X-ray spectrometer (EDS) and N_2 adsorption–desorption measurements. The results indicated that the complex photocatalyst prepared with a molar ratio of Brij98:CTAB=1:1 showed a uniform pore size of ca. 7 nm and a high specific surface area (S_{BET}) of 279.0 $m^2 g^{-1}$, and exhibited the highest photocatalytic activity for degradation of papermaking wastewater under ultra-violet light irradiation. The chemical oxygen demand ($CODc_r$) percent degradation was about 73% in 12 h and chroma percent degradation was 100% in 8 h.

1. Introduction

Mesoporous materials have exhibited many potential applications in industrial catalytic reactions, because they have high surface area, large pore size, multidimensional framework and reusability [1]. Mesoporous titania as one of the most promising photocatalysts has been widely investigated for its advantages such as high efficiency, good stability, ready availability, and nontoxicity [2–5]. In fact, more attention has been paid to the control size and shape of primary particles as well as manipulation of their arrangement and network structure. In particular, incessant attempts have focused on tailoring the mesoporous network with high surface area because this type of network structure could promise optimal performance in photoresponsive applications such as photocatalysis and dye-sensitized solar cells [6]. The mesoporous structure with high surface area could provide not only easy accessibility of guest molecules to active sites but also more chances to receive both light and guest molecules. Therefore, several attempts have been recently made to realize the mesoporous transition metal oxides by using organic templates such as phosphates and amines, which resulted in specific surface area [7,8].

The main wastewater treatment process used in papermaking industry is primary clarification, followed by the second treatment, generally of a biological nature. But the effluent after a biological treatment still contains appreciable concentrations of chemical oxygen demand (COD), color, and toxicity [9]. The COD that originates from persistent substances in the wastewater cannot be further reduced by biological process alone. The color components are lignin and lignin derivates which exist in the form of colloidal particles. If the treated effluent is discharged into water streams or land mass without further treatment, it will result in severe environmental pollution [10,11]. In addition, the papermaking industry is likely to face more stringent regulations on the quality of effluents entering receiving water. Thus, the use of tertiary treatment for papermaking wastewater has to be considered in the future. Among the various advanced oxidation processes that have been proposed for the degradation of recalcitrant azo-dyes, TiO_2-mediated photocatalysis has been shown to be potentially advantageous as it may lead to complete mineralization of pollutants to CO_2, water, and mineral acids [12].

In this article, a straightforward combined sol–gel process with surfactant-assisted templating method [13] was reported as a potential technique for co-doped mesoporous TiO_2 synthesis. The photocatalytic activities of co-doped mesoporous TiO_2 materials prepared from different molar ratios of composite surfactant templates have been tested via heterogeneous photocatalytic degradation of papermaking wastewater under UV light irradiation.

2. Experimental

2.1. Chemicals

Polyoxyethylene (20) oleyl ether (Brij98, $C_{18}H_{35}(OC_2H_4)_{20}OH$), cetyl trimethyl ammonium bromide (CTAB, $C_{16}H_{33}(CH_3)_3NBr$) and tetrabutyl titanate (TBT) were purchased from Aldrich. Titanium

* Corresponding author. Fax: +86 531 89631625.
E-mail address: guoweizhou@hotmail.com (G. Zhou).

0022-4596/$ - see front matter © 2010 Elsevier Inc. All rights reserved.
doi:10.1016/j.jssc.2010.04.016

dioxide powder P-25 was purchased from Degussa Co. (Germany). Lanthanum nitrate hexahydrate, urea, ethanol, and glacial acetic acid were analytical grade and used as received without further purification.

2.2. Photocatalysts preparation

Co-doped mesoporous titania photocatalysts were prepared by the sol–gel method. First, 34.03 g TBT was dissolved in 79 g anhydrous ethanol with constant stirring to form solution A. Into the solution specified amounts of Brij98 and CTAB, with molar ratios of Brij98:CTAB ranging from 1:2 to 2:1, were added dropwise for the preparation of a set of samples. Second, 0.52 g lanthanum nitrate hexahydrate and 0.06 g urea were dissolved in 90 g deionized water at room temperature, followed by adding 10.49 g glacial acetic acid to obtain solution B. Then, solution A was added dropwise into solution B within 60 min under vigorous stirring. Subsequently, the obtained sol was stirred continuously for 2 h and aged for 48 h at room temperature. Then the resulting white gel was dried at 80 °C for 3 h to give a yellow xerogel. After grinding, the as-synthesized materials were calcined at 400 °C for 4 h in a tube furnace to remove the surfactant templates.

2.3. Photocatalysts characterization

X-ray diffraction (XRD) patterns were recorded on a D8 advance diffractometer (Bruker Company) using Cu $K\alpha$ radiation (40 kV, 40 mA, $\lambda=0.15406$ nm). The data were collected from 20° to 70° with a resolution step size of $0.1^\circ s^{-1}$. The sample morphology was observed by a transmission electron microscope (TEM, HITACH H-800) at an acceleration voltage of 200 kV. Fourier transformed infrared (FT-IR) spectra were taken in a Bruker Tensor 27 instrument. The resolution and scan number were $4\,cm^{-1}$ and 32, respectively. The element mappings over the desired region of the photocatalysts were detected by an energy-dispersive X-ray spectrometer (EDS) attached to the scanning electron microscope (SEM, Quanta ESEM Felco-Holland). Nitrogen adsorption–desorption isotherms of the materials were determined at −196 °C by a conventional volumetric technique with a Coulter Omnisorp 100CX sorption analyzer. Each sample was degassed at 350 °C for 6 h under a pressure of 10^{-5} Pa or less. The surface areas were calculated by the Brunauer–Emmett–Teller (BET) method in the relative pressure range of $P/P_0=0.05$–0.25. The pore size distributions were evaluated from the adsorption branches of isotherms by using the classical Barrett–Joyner–Halenda (BJH) model, which applies for cylindrical pores.

2.4. Determination of photocatalytic activity

The photocatalytic activities of N, La co-doped mesoporous TiO_2 materials prepared here were measured by photodecomposition of black liquid from pulping and papermaking under UV light irradiation. The photodegradation reaction was carried out in a cylindrical quartz reactor, which had water circulation facility at the outer wall of the reactor. A 375 W high pressure mercury lamp was used as the UV light source. The distance between reactant and light source was fixed at 20 cm. Prior to the reaction, 200 mL of black liquid from pulping and papermaking (initial $CODc_r=500\,mg\,L^{-1}$, pH=5.0) and 0.2 g photocatalyst were mixed by ultrasonic dispersion in dark. After the mixture suspension was ultrasonicated for 20 min to achieve the adsorption equilibrium, the lamp was then turned on. During irradiation, the suspension was vigorously stirred with a magnetic stirrer and bubbled with oxygen at a constant flow rate. At regular time intervals, 10 mL of the suspension was periodically taken out and centrifugated at 6000 rpm for 15 min. The obtained solution was measured to check the residual concentration of the black liquid with a UV-vis spectrophotometer at 280 nm, which is the maximum absorption of the black liquid. According to the transformation of absorbance before and after illumination, the percent degradation of black liquid can be calculated as follows: $(A_0–A)/A_0\times100\%$, where A_0 is the absorbance of initial black liquid and A is the absorbance after illumination. The measurements were repeated three times for each photocatalyst which was drawn from one batch of material and the results were averaged. COD measurements were carried out by the dichromate titration method (referred to as $CODc_r$); chroma measurements were carried out using the CPPA standard method [11,14].

3. Results and discussion

3.1. X-ray diffraction characterization

The phase structure, crystallite size and crystallinity of TiO_2 play an important role in photocatalytic activity. Many studies have confirmed that the anatase phase of titania shows higher photocatalytic activity than the brookite or rutile phase [15]. From the wide angle XRD patterns (Fig. 1), the titania samples exist only in anatase phase, with their characteristic diffraction peaks of 2θ values at about 25.4° (101), 37.9° (004), 48.0° (200), 54.0° (105), 54.9° (211) and 62.8° (204), respectively. The anatase phase of the samples did not change before and after using Brij 98/CTAB, illustrating that Brij98 and CTAB did not change the catalysts structure and retained the good anatase crystallization [16]. The average size of the crystallite was estimated based on the broadening of (101) peak at $2\theta=25.4^\circ$ using the Scherrer equation [17], $D=k\lambda/B\cos\theta$, where k is a shape factor of the particle, λ and θ are the wavelength and the incident angle of the X-rays, respectively, and B is the full width at half maximum (FWHM) of the 2θ peak. The crystallite sizes are shown in Table 1. It can be seen that the average crystallite size of mesoporous TiO_2 is about 10 nm, which is smaller than that (15.6 nm) of the nano TiO_2 prepared without surfactant. Among all the mesoporous TiO_2, the sample prepared with molar ratio of Brij98:CTAB=1:1 shows the smallest crystallite size (9.6 nm). The smaller crystallite size indicates that the preparation method used

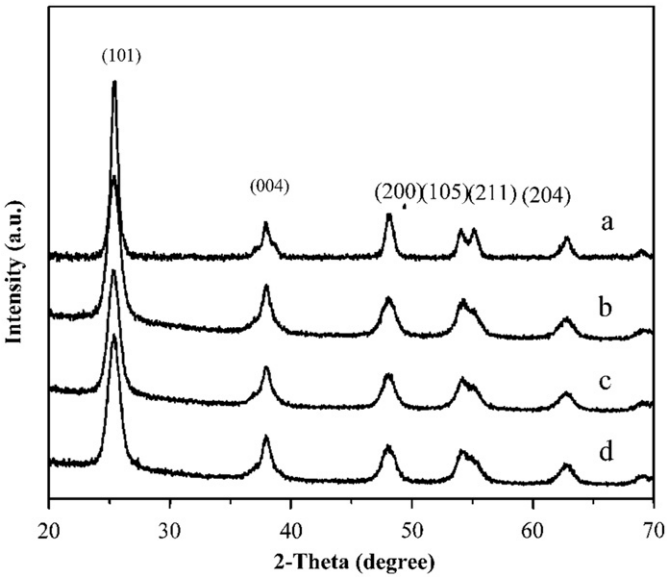

Fig. 1. XRD patterns of N, La co-doped TiO_2 samples prepared with different molar ratios of Brij98:CTAB. (a) 1:1, (b) 1:2, (c) 2:1, and (d) 0:0.

Table 1
Structural parameters of the mesoporous TiO_2 on a composite template.

Brij 98:CTAB molar ratio	Crystallite size (nm)[a]	S_{BET} ($m^2 g^{-1}$)[b]	Pore size (nm)[c]	V_p ($cm^3 g^{-1}$)[c]
0: 0	15.6	75.94	–	–
1: 1	9.60	279.0	4.4 and 7.0	0.30
1: 2	11.0	267.1	4.6 and 6.9	0.30
2: 1	10.3	258.4	4.5 and 6.8	0.29

[a] Average crystallite size of TiO_2 was determined by XRD using the Scherrer equation.
[b] The BET surface area was determined by the multipoint BET method using the adsorption data in the relative pressure (P/P_o) range of 0.05–0.25.
[c] Pore volume and average pore size were determined by nitrogen adsorption volume at the relative pressure of 0.99.

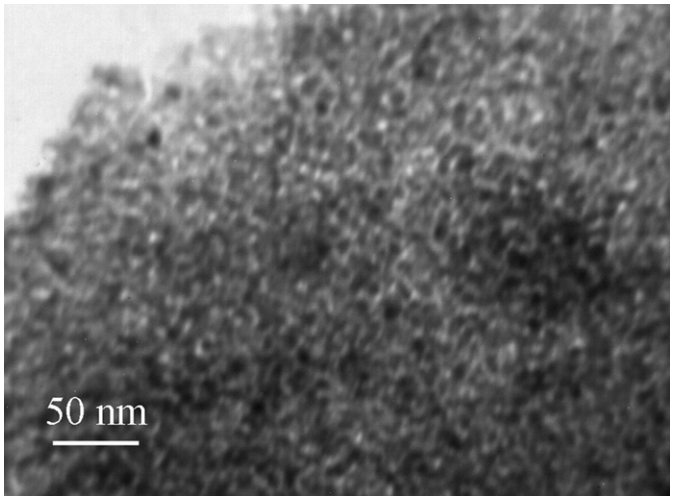

Fig. 2. TEM image of N, La co-doped mesoporous TiO_2 sample prepared with a molar ratio of Brij98:CTAB=1:1.

in the present work can effectively prompt the crystallization and inhibit the grain growth.

3.2. Transmission electron microscopy characterization

Fig. 2 presents the TEM image of the N, La co-doped mesoporous TiO_2 sample prepared with a molar ratio of Brij98:CTAB=1:1. The sample has a disordered wormhole-like pore structure. The accessible pores are randomly connected, lacking of discernible long-range order in the pore arrangement among the small TiO_2 particles. The mean mesopore size is ca. 6–7 nm, which is in good agreement with the pore size calculated from N_2 isotherms.

3.3. Infrared characterization

As shown in Fig. 3, the bands at 3238 and 3356 cm^{-1} are assigned to N–H stretching vibration and O–H stretching vibration of the adsorbed water on the surface of the materials [18,19]. The stronger peaks at 1622 and 1625 cm^{-1} are attributed to the hydroxyl groups bending vibration of O–H on the catalysts. The small peak at 1481 cm^{-1}, produced by $-NO_x(-Ti-O-N-Ti)$, indicates that some nitrogen atoms in the mesoporous TiO_2 sample existed in the form of $-NO_x$ [20]. This is consistent with the result of N-doped TiO_2 reported by Chen et al. [18], who reported that the nitrogen incorporation produced an N–O

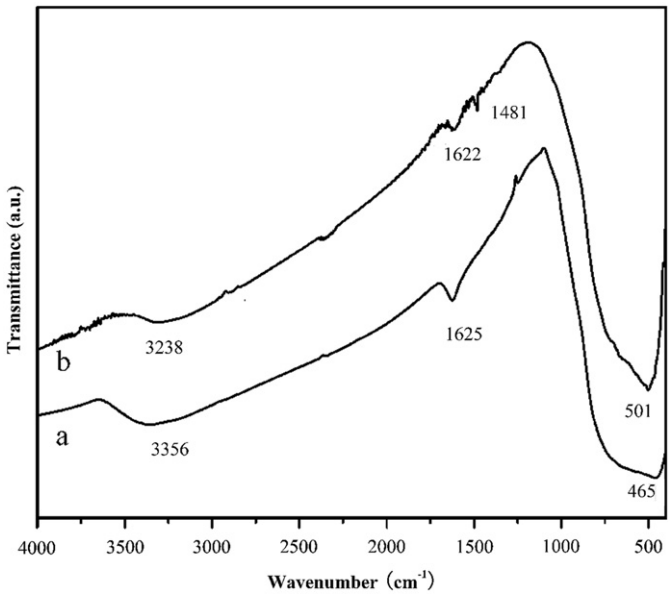

Fig. 3. The FT-IR spectra of (a) pure TiO_2 and (b) N, La co-doped TiO_2 prepared with a molar ratio of Brij98:CTAB=1:1.

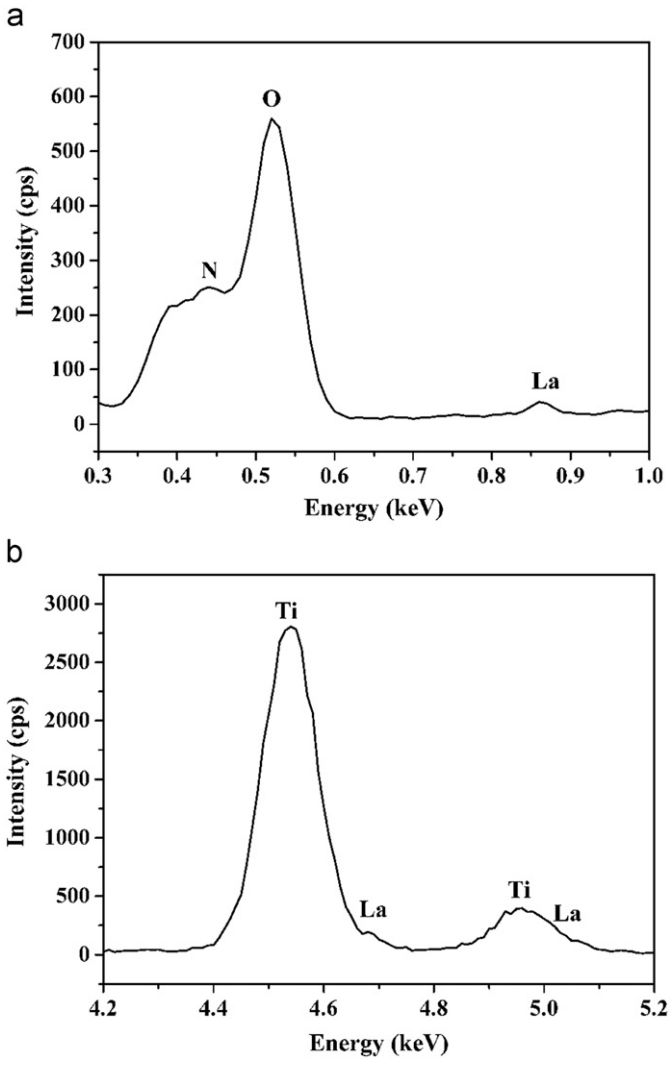

Fig. 4. EDS analysis of N, La co-doped mesoporous TiO_2 sample prepared with a molar ratio of Brij98:CTAB=1:1. (a) N, O, and La and (b) Ti and La.

bonding region. Low frequency bands at 465 and 501 cm^{-1} are aroused by the stretching vibration of Ti–O [18,21]. Upon addition of La^{3+}, a small shift of about 36 cm^{-1} to higher frequencies could be detected for the stretching vibration of Ti–O.

3.4. Energy-dispersive X-ray spectrometer characterization

The EDS analytical results (Fig. 4) show that N, La co-doping elements in the modified TiO_2 are well distributed within TiO_2 grains. For mesoporous TiO_2 sample prepared with a molar ratio of Brij 98:CTAB=1:1, the molar ratios of O/Ti, N/Ti, and La/Ti are 1.51, 0.26, and 0.089, respectively. This is because parts of oxygen in the samples are substituted by nitrogen atoms. The peak at ca. 0.43 keV was attributed to N. There are different peaks formed by La at ca. 0.87, 4.68, and 5.07 keV. These results may confirm the incorporation of lanthanum and nitrogen into TiO_2.

3.5. Porosity characterization

Fig. 5 shows the nitrogen adsorption–desorption isotherms and the corresponding BJH pore size distributions of the samples with different molar ratios of composite surfactant templates. The mesoporous TiO_2 prepared at composite surfactant templates exhibited type IV isotherms with H2 hysteresis loops (Fig. 5a–c, IUPAC classification), which are related to the mesoporous structure. A clear hysteresis loop with a sloping adsorption branch and a relatively sharp steep desorption branch were observed at a high relative pressure (P/P_o) range. The adsorption isotherm of the as-prepared sample exhibits a large increase in the P/P_o range of 0.5–0.8, which is related to the capillary condensation associated with large pore channels. The nano TiO_2 prepared at a molar ratio of Brij98:CTAB=0:0 exhibited a different isotherm from the former three. The BET surface area, pore parameter, and pore volume of the mesoporous TiO_2 samples are summarized in Table 1. The BET surface areas of the mesoporous TiO_2 samples decreased, however, from 279.0, 267.1–258.4 $m^2 g^{-1}$, accompanied with the decrease of pore volumes from 0.30 to 0.29 $cm^3 g^{-1}$. The BET surface area of nano TiO_2 sample prepared at a molar ratio of Brij98:CTAB=0:0 was only 75.94 $m^2 g^{-1}$. The BJH calculation for pore-size distribution from the desorption data reveals a bimodal distribution centered at ca. 4.5 and 6.9 nm. On the other hand, adsorption data gave only one pore size maximum at 6.9 nm associated with the emptying of framework pores at values between $P/P_0=0.1$ and 0.4. The small pore sizes (4.5 nm) are a reflection of the step near $P/P_0=0.5$ on the desorption branch and correspond to the emptying of textural pores.

3.6. Photocatalytic activity

Photocatalytic decomposition of black liquid from pulping and papermaking under UV light irradiation was used to investigate the properties of the synthesized mesoporous materials. Contrast experiments results show that the chroma and $CODc_r$ values of black liquid from pulping and papermaking were almost not changed in the dark. The observed results during photocatalytic decomposition of papermaking wastewater under UV light irradiation in the presence of mesoporous TiO_2 and P-25 are shown in Fig. 6.

$CODc_r$ values are related to the total concentration of organic pollutant in wastewater and the changes in $CODc_r$ percent degradation reflect the degree of mineralization of organic pollutant as a function of irradiation time. Preliminary series of experiments were carried out in order to determine the optimum amounts of Brij98 and CTAB. It was found that N, La co-doped mesoporous TiO_2 showed a good photocatalytic activity in the degradation of papermaking wastewater. $CODc_r$ percent

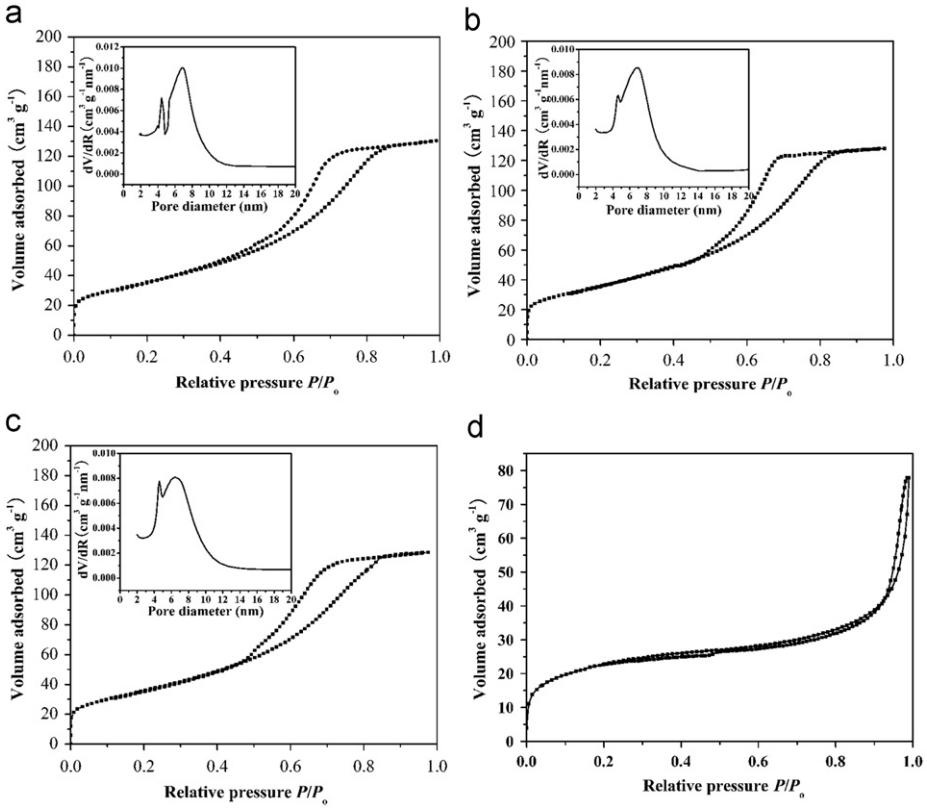

Fig. 5. Nitrogen adsorption–desorption isotherms and the corresponding BJH pore size distributions (insets) from the adsorption branches for the calcined samples at different molar ratios of Brij98:CTAB. (a) 1:1, (b) 1:2, (c) 2:1, and (d) 0:0.

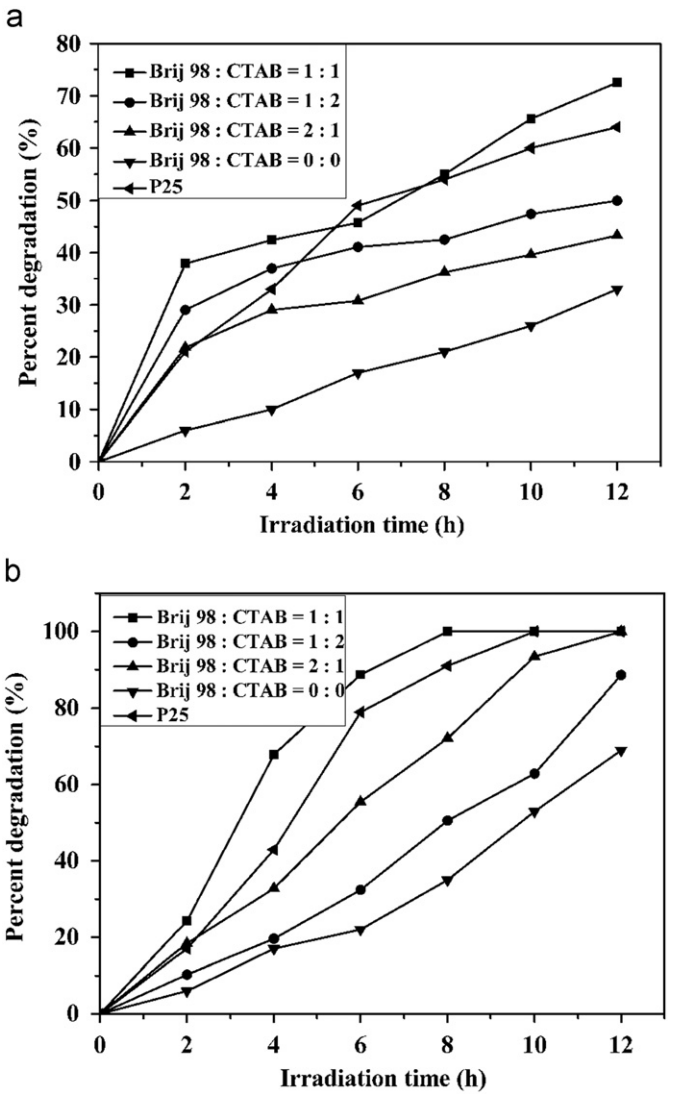

Fig. 6. Percent degradation of (a) $CODc_r$ and (b) chroma of papermaking wastewater in the presence of mesoporous TiO_2 and P-25 as a function of UV light irradiation time.

degradation is about 73% after a period of 12 h and chroma percent degradation is 100% within 8 h over the sample prepared with a molar ratio of Brij98:CTAB = 1:1. The percent degradation of $CODc_r$ and chroma of papermaking wastewater over the mesoporous TiO_2 prepared with a molar ratio of Brij98:CTAB = 1:1 was found to be higher than that for the Degussa P25. Besides the benefit of photocatalytic activity enhancement, these mesoporous materials can be separated from the suspension solution more easily than pure TiO_2 nanoparticles [22].

From the photocatalytic results, one can find that photocatalytic activity of mesoporous titania is strongly dependent on its phase structure, crystallite size, specific surface area, and pore structure. It is seen from XRD spectra that the mesoporous TiO_2 phase structure did not change before and after using Brij 98/CTAB, and retained the good anatase crystallization. The crystallite size of TiO_2 decreased from 15.6 to 9.60 nm after using Brij98 and CTAB, which may benefit their photocatalytic performance. The mesoporous TiO_2 samples with various specific surface areas exhibited different photocatalytic degradations for the wastewater [23]. Among them, the sample prepared with a molar ratio of Brij98:CTAB = 1:1 exhibited a slightly higher surface area ($279.0\,m^2\,g^{-1}$) than others and the highest $CODC_r$ percent degradation (73%) and chroma percent degradation (100%). For the samples with higher specific surface area, most of the molecules were adsorbed on the edge of the TiO_2 micropores where they could easily migrate to the TiO_2 surface. After being captured by photogenerated oxidizing species, it degraded immediately. As the specific surface area and pore volume increased, the adsorption capacity increased. Since this sample might provide a medium adsorption for the organics, followed by transfer to TiO_2 surface where they were degraded completely, the kinetic equilibrium between adsorption and photodegradation of wastewater was then reached. In other words, an increase in adsorption favored the degradation of the wastewater. Therefore, it can be concluded that the surface area and pore structure of this sample had an important effect on its degradation efficiency for wastewater from the papermaking industry. The surface area may be moderate for organic molecules from papermaking wastewater, and the best synergistic effect between adsorption and photocatalysis has been reached [24].

4. Conclusions

N, La co-doped mesoporous TiO_2 materials with uniform pore size and large specific surface area were successfully synthesized using composite surfactant templates (Brij98/CTAB) as the structure-directing agents. XRD patterns showed that the dominant crystal type of prepared TiO_2 was anatase. TEM image and N_2 adsorption–desorption isotherms analysis revealed the mesoporous co-doped TiO_2 materials with an average size of 6–7 nm and a high specific surface area of $258.4–279.0\,m^2\,g^{-1}$. N, La co-doped mesoporous TiO_2 showed a good photocatalytic activity in the degradation of papermaking wastewater. $CODc_r$ percent degradation was about 73% in 12 h and chroma percent degradation was 100% in 8 h under UV light irradiation for the sample prepared at the molar ratio of Brij 98:CTAB = 1:1.

Acknowledgments

The work described in this paper was financially supported by the National Natural Science Foundation of China (Grant No. 20976100) and the Key Project of Natural Science Foundation of Shandong Province (Grant No. Z2006B07).

References

[1] H.Y. Hao, J.L. Zhang, Micropor. Mesopor. Mater. 121 (2009) 52–57.
[2] W.S. Chae, S.W. Lee, Y.R. Kim, Chem. Mater. 17 (2005) 3072–3074.
[3] P. Sudhagar, R. Sathyamoorthy, S. Chandramohan, Appl. Surf. Sci. 254 (2008) 1919–1928.
[4] J.G. Yu, X.J. Zhao, J.C. Du, W.M. Chen, J. Sol–Gel Sci. Technol. 17 (2000) 163–171.
[5] D.S. Kim, S.J. Han, S.Y. Kwak, J. Colloid Interface Sci. 316 (2007) 85–91.
[6] K. Kalyanasundaram, M. Graetzel, Coord. Chem. Rev. 77 (1998) 347–414.
[7] S.M. Paek, H. Jung, Y.J. Lee, M. Park, S.J. Hwang, J.H. Choy, Chem. Mater. 18 (2006) 1134–1140.
[8] T. Sreethawong, Y. Suzuki, S. Yoshikawa, J. Solid State Chem. 178 (2005) 329–338.
[9] R.S. Yuan, R.B. Guan, P. Liu, J.T. Zheng, Colloids Surf. A 293 (2007) 80–86.
[10] W.L. Sun, Y.Z. Qu, Q. Yu, J.R. Ni, J. Hazard. Mater. 154 (2008) 595–601.
[11] M. Pérez, F. Torrades, J. Peral, C. Lizama, C. Bravo, S. Casas, J. Freer, H.D. Mansilla, Appl. Catal. B 33 (2001) 89–96.
[12] M. Stylidi, D.I. Kondarides, X.E. Verykios, Appl. Catal. B 47 (2004) 189–201.
[13] T. Sreethawong, Y. Suzuki, S. Yoshikawa, Catal. Commun. 6 (2005) 119–124.
[14] Chinese National Standard, GB 11914-89, 1989.
[15] M. Grandcolas, M.K.L. Du, F.B.A. Louvet, N. Keller, V. Keller, Catal. Lett. 123 (2008) 65–71.
[16] J.X. Li, J.H. Xu, W.L. Dai, H.X. Li, K.N. Fan, Appl. Catal. B 82 (2008) 233–243.
[17] Y.Y. Wang, G.W. Zhou, T.D. Li, W.T. Qiao, Y.J. Li, Catal. Commun. 10 (2009) 412–415.
[18] X.B. Chen, Y.B. Lou, A.C.S. Samia, C. Burda, J.L. Gole, Adv. Funct. Mater. 15 (2005) 41–49.
[19] B. Wawrzyniak, A.W. Morawski, Appl. Catal. B 62 (2006) 150–158.

[20] D.G. Huang, S.J. Liao, W.B. Zhou, S.Q. Quan, L. Liu, Z.J. He, J.B. Wan, J. Phys. Chem. Solids 70 (2009) 852–859.
[21] Y.L. Shen, Mater. Sci. Eng. A 237 (1997) 102–108.
[22] X. Zhang, H. Yang, F. Zhang, K.Y. Chan, Mater. Lett. 61 (2007) 2231–2234.
[23] Y. Yang, Y.H. Guo, C.W. Hu, Y.H. Wang, E.B. Wang, Appl. Catal. A 273 (2004) 201–210.
[24] Y. Liu, D.Z. Sun, L. Cheng, Y.P. Li, J. Environ. Sci. Health. Part A: Toxic/Hazard. Subst. Environ. Eng. 18 (2006) 1189–1192.